Photocatalysis of Bispyribac Sodium in Water under Direct Sun Light Using ZnO Nano Particles: Kinetics and Toxicity of Breakdown products

Naveetha Gaggara[*]**, Atmakuru Ramesh**

Department of Analytical Chemistry, International Institute of Biotechnology and Toxicology (IIBAT),
Padappai, Chennai 601 301, Affiliated to the University of Madras, Tamil Nadu, India
*Corresponding author: navi.chem86@gmail.com

Abstract The present research describes the photo catalytic degradation of Bispyribac sodium, a pyrimidinyloxybenzoic herbicide, widely used in the protection of the paddy field. The degradation was investigated in an aqueous suspension using $ZnO/Na_2S_2O_8$ as the photo sensitizer / oxidant. Photocatalysis of bispyribac sodium was studied in three different aqueous buffer solutions (pH 4, 7 and 9) under direct sunlight. Liquid Chromatography Electro spray Tandem Mass spectrometry (LC-MS/MS) was used to identify the major photo transformation products in water. In this present study we also investigated the effect of bispyribac sodium and its breakdown products on the growth of green alga *(Pseudokirchneriella subcapitata)*. The results showed that the addition of a photosensitizer was strongly enhancing the elimination of pesticides when compared to photolysis tests. This process also enhances the reaction rate very rapidly. The addition of the oxidant $(Na_2S_2O_8)$ with the ZnO increases the rate of reaction has the added advantage over the ZnO alone. The degradation of the bispyribac Sodium follows first order kinetics. Green alga growth rates (E_r) and yield percentage (E_y) were determined statistically. Initially, the growth rate inhibition was very high after that the inhibition was decreased while increasing the irradiation Time.

Keywords: *zinc oxide, nanoparticles, oxidant, photosensitizer, herbicide, Green alga*

Cite This Article: Naveetha Gaggara, and Atmakuru Ramesh, "Photocatalysis of Bispyribac Sodium in Water under Direct Sun Light Using ZnO Nano Particles: Kinetics and Toxicity of Breakdown products." *Applied Ecology and Environmental Sciences*, vol. 8, no. 1 (2020): 1-11. doi: 10.12691/aees-8-1-1.

1. Introduction

Surface water contamination is a major public health hazard issue due to the extensive use of crop protection chemicals in agriculture**.** Herbicide residues are likely to get transferred to aquatic reservoirs by surface runoff and leaching. Photo catalytic degradation is one of the important factors contributing to the rapid dissipation of agrochemicals in water. Photo-catalysis is widely used in the industry for the effective decontamination of large quantities of effluents and other wastages to protect the environment and human health [1-12]. In recent years, researchers have identified nanoparticles having different physical and chemical properties as catalysts, when compared to conventional materials due to the availability of larger surface area [13]. Nano-sized TiO_2 dominates the inorganic UV absorption phenomena for the photo-catalytic decontamination of organic pollutants. The nano-sized ZnO was used in similar applications at smaller volumes. The ZnO nanoparticles are known to promote the reactions in the presence of light and have the potential to accelerate the degradation rate due to photo-assisted oxidative mineralization of pesticides to carbon dioxide and water when exposed to UV irradiation/sunlight. The photocatalytic activity of both ZnO and TiO_2 catalysts was studied with acid brown 14 as the model pollutant. The highest photo degradation rate observed in ZnO, suggesting that it absorbs the large fraction of the solar spectrum and absorption of more light quanta than TiO_2 [14]. The photo catalytic activity of ZnO can be explained from the fact that when photons of a certain wavelength are incident upon its surface, electrons are promoted from the valence band and transferred to conductance band, thus leaving positive holes in the valence band, which react with the hydroxylated surface to produce OH radicals, which are the most potent oxidizing agents [15]. The comparison of the photo catalytic activity of zinc oxide and titanium dioxide in water samples contaminated with phenolic compounds. Among the pair, the zinc oxide exhibited higher activity than TiO_2 under artificial light radiation system [16]. The degradation of methomyl in water under UV radiation using TiO_2 and ZnO as catalysts shows the increase in the pH of the water reduces the degradation rate of the contaminant in the presence of photo catalyst [17]. A comparative study between ZnO nanoparticles and its gold coated Zinc oxide Nano rods in the decontamination of the Rhodamine A shows very fast degradation of contaminants

in the presence in gold-coated nanorods when compared to ZnO nanoparticles [18]. The photo catalytic degradation of 2, 4-D using flat plate reactor zinc oxide as a photo catalyst under UV irradiation it was observed that the time required to mineralize the residues in water and reported that 38.1% of mineralization occurred in 8 hours continuous treatment [19]. A comparative study between La-doped ZnO with pure ZnO and TiO_2 for the degradation of monocrotophos in aqueous solution. It shows that the degradation rate was increased with increase in the La content [20]. The photo catalytic activity of TiO_2 and ZnO on 2, 4- D in aqueous solution with an effect of pH and addition of H_2O_2 was investigated. The degradation of residues was faster with ZnO when comparing TiO_2 in the presence of hydrogen peroxide [21]. Photo catalytic degradation of sulfonylurea urea herbicides in water with ZnO as the catalyst [22,23] and the decontamination of 4-Chlorophenol in the presence of different anions and cations were studied [24,25] by UV induced photo-catalytic degradation. The Decontamination of the dye methylene blue under the influence of UV rays in water showed that the ZnO nanoparticles are better than its nanocrystalline form [26]. The photocatalytic activity of TiO_2 and ZnO are reported for the decontamination of polychlorinated dibenzo-p-dioxins [27], isothiazolin-3-ones [28] phosphamidon in water [29]. In several studies, it has been proven the similar efficiency of photocatalytic degradation between ZnO and TiO_2. Some of the reviewers concluded that ZnO nano particles are better substitute to TiO_2 in some applications; Therefore, ZnO can be a suitable alternative for TiO_2 [30,31,32]. Photo catalytic degradation of Phenol Red (PR) can also be observed by using ZnO nanomaterial as a photo catalyst. The study concluded that photo catalytic degradation of PR has only taken place in the presence of ZnO as the photo catalyst, without which it might have taken a very long period to degrade [33]. Literature survey revealed that Zinc oxide is one of the most important semiconductor materials today. And these are having a wide range of applications in different industries because of its optical and electronic properties. ZnO and TiO_2 have the same band gap (3.37 eV) and ZnO is most abundant and less in cost [34]. For these reasons, ZnO particles have been used to degrade different organic and pesticide contaminants in water.

Bispyribac Sodium is a broad- spectrum herbicide used to controls annual and perennial grasses, broadleaf weeds and sedges in Paddy field. It is relatively high solubility in water (73.3 g/L at 25°C), and the compound is very stable against photolysis [35]. Its chemical stability of the parent and the metabolites along with its mobility enables this herbicide to cause contamination of the ground water via leaching through the soil as well as surface water supplies via dissolved run-off and erosion [36]. It was considered as "not readily biodegradable" according to a standard test [37] of ready biodegradability following incubation with an activated sludge inoculum. Based on environmental fate properties and its mobility it leads to ground water contamination. It has the potential to bio-accumulate in aquatic organisms from the above literature review about the persistence nature of the bispyribac sodium, we have developed effective detoxification methods for eliminating these pesticides from water.

This present work is mainly aimed at the determination of photo catalytic degradation of the herbicide, bispyribac sodium by using ZnO / $Na_2S_2O_8$ as catalyst/oxidant in different water media. From the above information, the present study is conducted with an objective to establish the conditions for photo catalytic activity of ZnO nanoparticles in the decontamination of very persistent herbicide of Bispyribac sodium in water. The effects of initial concentration of the compound, the amount of catalyst used and the addition of an oxidant to the photo catalysis were studied. In addition to this detoxification of the degradation products to aquatic species (Fresh water alga i.e. *Pseudokirchneriella subcapitata*) was investigated.

2. Materials and Methods

2.1. Materials

Bispyribac sodium (99.9%), analytical reference standard- Aldrich (USA), HPLC grade Acetonitrile (99.9%) – Merck Limited, Mumbai, Sodium persulfate (98%) - Merck Limited, Mumbai, Ortho–phosphoric acid (85%) - Merck Limited, Mumbai, Potassium biphthalate (99.5%) - Merck Limited, Mumbai, Sodium phosphate dibasic (99.5%) - Merck Limited, Mumbai, Potassium Phosphate (99.5% -100.5%) - Merck Limited, Mumbai, Sodium Tetra borate (99.5%), Zinc acetate dihydrate (99.0%), Triethanol amine (99.8%), Ethanol (90.%), and ammonium hydroxide (50%) was obtained from the Merck India Limited, Mumbai. Distilled water was purified using the Milli-Q Plus apparatus (Millipore, Bedford, MA, USA).

2.2. Methods

2.2.1. Preparation of ZnO nano particles

20 mL of double distilled water was taken in to a 100 mL beaker and 30 mL of triethanolamine was taken, to this ethanol was added drop wise (2 mL) with continuous stirring results a homogeneous solution (Solution-I). 0.5 M Zinc acetate di hydrate solution was prepared by adding 5.42 g of Zinc acetate in 50 mL of water subjected to continuous stirring to get a homogeneous solution (Solution-II). Now, these two solutions were mixed in a 500 mL beaker, and ammonium hydroxide was added with continuous stirring and heating for 20 minutes. The resulting solution is in the form of a yellow colored gel. Then the gel was washed 5-7 times with water and dried in a hot air oven at a temperature of about 200°C for 8 hours. The obtained powder was calcinated at 700°C for four hours [38].

2.2.2. Preparation of Bispyribac Sodium Stock Solution

Stock solutions (1000 mg L^{-1}) of the pesticide standard were prepared in acetonitrile protected from light and stored at 5°C. An intermediate stock solution was prepared by dilution in the same solvent to obtain a concentration of 10 mg L^{-1}. Several standard solutions with the concentration of 0.01-2.0 mg L^{-1} were injected to

obtain the linearity of detector response and detection limits of pesticide studied.

2.3. Preparation of Different pH Buffers

pH 4 - Dissolved 40 g of Potassium dihydrogen Phosphate in 5000 mL of distilled water. The pH was adjusted to 4.0 using potassium dihydrogen phosphate

pH 7 - Dissolved 31.5 g of disodium hydrogen orthophosphste and 25.0 g of Potassium dihydrogen phosphate in 5000 mL of distilled water. pH was adjusted to 7.0 using disodium hydrogen ortho phosphate and porassim dihydrogen phosphate.

pH 9 - Dissolved 62.5 g of boric acid and 75.0 g of potassium chloride in 5000 mL of distilled water. pH was adjusted to 9.0 using sodium hydroxide.

2.4. Preparation of Nutrient Stock Solution

The Nutrient medium was prepared dissolving known quantity of each nutrient according to OECD TG 201. The Pre-culture of *Pseudokirchneriella subcapitata* Strain SAG 61.81, the Primary culture obtained from University of Gottingen, Germany and the culture was maintained in the department of Ecotoxicology, IIBAT as per OECD Guideline [39]. Pre-culture of *Pseudokirchneriella subcapitata* was prepared three days before initiation of the study. The inoculated flasks were kept in the shaker incubator with rpm of 110 - 116 and maintained with the continuous illumination of 6618-6753 lux light intensity at 22.1 to 23.4°C for three days. The alga cell count was examined in all the flasks by using Improved Neubaur's Haemocytometer under illuminance of the microscope.

2.5. Photo Catalysis Procedure

The photo catalysis of Bispyribac sodium in water was studied by spiking Bispyribac sodium standard at 10 mg L^{-1}. The study was conducted in aqueous buffer solutions of pH 4.0, 7.0 and 9.0. Three replications were made at each fortification level along with control (Milli-Q Water) samples for comparison. Two sets of spiked concentrations are prepared for the studies. In one set of samples, the catalyst Zinc oxide nanoparticles and sodium persulphate were added at 150 mg L^{-1}, and 100 mg L^{-1} and the other set was studied without the addition of catalyst and oxidant ($Na_2S_2O_8$). The samples were exposed to direct sunlight. Aliquots of samples were collected at pre-determined intervals. Several samples were collected at (0, 5, 10, 20, 50, 70, 90, 120, 150,180,200 and 250 h). The temperature of water samples during the period was 25 to 44°C. The sunlight intensity at the time of photoperiod was 20000-170000 Lux. The samples were collected on different sampling occasions were filtered using 0.2 µm PTFE membrane filter and collected the filtrates into amber colored vials. The samples fortified with Zinc oxide nanoparticles were centrifuged using Beckman cooling centrifuge at 10000 rotations per minute for 4 minutes at 2°C. The supernatant was transferred into the amber-colored vials and stored in the dark at 5°C, up to the analysis to avoid further degradation of the compound.

2.6. Procedure for Toxicity Assessment of Bispyribac Sodium to Green Alga

To the above culture photo catalysis, sample was spiked at the concentration of 10 µg/mL (diluted to10 folds) in the OECD medium (1µg/mL). The pH was measured and adjusted to 8.0 ± 0.1 using 0.1N NaOH. In 250 mL Erlenmeyer flasks 100 mL of the test solution was transferred. Three replicates and one control were maintained for the test. The control and treated flasks were inoculated with 100 µL of *Pseudokirchneriella subcapitata* from the pre-culture to obtain an initial cell concentration of approximately 1×10^4 cells per mL. The pH was recorded at test termination. From this experiment alga Cell count, percent inhibition of the yield (% Iy) and the percentage inhibition of average specific growth rate (% I_r) at each test duration was calculated using software ECOSTATS Program version 2012.06.03 (SAS version 9.3, SAS Institute Inc., Cary, NC, 2002-2010).

The yield was calculated using the following formula

$$Y_{i-j} = X_j - X_i$$

Where,
Y $_{i-j}$ = biomass from the start of the test to the end of the test
X_i = biomass (cells/mL) at time i (0 hour)
X_j = biomass (cells/mL) at time j (72 hours)

The percent inhibition of the yield (% Iy) at test concentration was calculated as,

$$\% \, Iy = (YC - YT)/YC \times 100$$

Where,
% Iy = percent inhibition of yield
Yc = mean value for yield in the control group
YT = value for yield for the treatment replicate.

The percentage inhibition of average specific growth rate at each test concentration (%I_r) was calculated as,

$$\% I_r = (\mu_C - \mu_T)/\mu_C \times 100$$

where,
% I_r is the percentage inhibition in average specific growth rate, $\mu_{C \, is}$ mean value for average specific growth rate (µ) in the solvent control group and μ_T is the average specific growth rate (µ) for the treatment replicate.

2.7. Instrumentation

The quantification of residues of bispyribac sodium was done by using Shimadzu High Performance Liquid Chromatography with UV detector. The column used was Agilent eclipse XDB-C18 (150m x 4.6 mm diameter x 3.5µ particle size) for bispyribac sodium. The eluent used was (ACN: 0.1% H_3PO_4) (50:50 v/v) and the flow was 1 mL min^{-1}, the wavelength was 246 nm. The volume injected was 10 µL and for elution time was 6.1 minutes respectively.

The fraction of photo irradiated samples were analyzed periodically for the confirmation of the breakdown products using a QQQ LCMS/MS interfaced with Mass Analyst instrument control and data processing software supplied by AB Sciex API 6500 used. Nebulizing gas and

drying gas was generated from the pressurized air using a Nitrox UHPLCMS nitrogen generator. The curtain gas flow rate was: 40, Nebulizing gas flow was 3.0, gas 1: 45, and gas 2: 50 and Temperature was 450°C. The scan range was 100 - 500 m/Z. The residues were separated using an Agilent 1290 infinity HPLC system with stationary phase Agilent Eclipse XDB C18 (150 mm, 4.6 mm i.d, and 5 µm particle size), gradient elution of 0.7 mL per minute containing 0.1% formic acidic in acetonitrile as mobile phase A and 0.1% formic acid in Milli - Q water was used as mobile phase B . The 35% to 65% flow program was used for the separation of herbicides. The volume injected was 10µL.

2.8. Data Analysis

2.8.1. Method Validation

The specificity, Linearity, precision and accuracy of the assay were determined to validate the method of bispyribac sodium. To check the precision five replicate determinations were used. To determine the linearity of bispyribac sodium, different known concentrations of (10.0, 2.0, 1.0, 0.5, 0.1, 0.05 and 0.01 mg L^{-1}) were injected. The specificity of the method was confirmed by injecting the mobile phase, acetonitrile, diluting solvents and buffer solutions. The correlation coefficient was calculated from the plot against the concentration of the standards versus the observed area. Based on a signal to noise ratio of 3:1, the limit of detection (LOD) of the instrument was established.

2.8.2. Recovery, Limit of Quantification and Repeatability

The recovery of residues from the three different buffer solutions was examined by fortifying a known concentration (0.05 mg L^{-1}) limit of quantification [LOQ] and 0.5 mg L^{-1} (LOQ x 10 level). The samples were homogenized using a homogenizer after fortification of the standard. They were then filtered, and residues of bispyribac sodium in the samples were analyzed with the HPLC-DAD method. Based on the results, the LOQ was established as 0.05 mg L^{-1}. The repeatability of the method showed an acceptable RSD % according to the Hurwitz equation below:

$$RSD\% < 2^{(1-0.5\ logC)} \times 0.67,$$

Here C is the concentration of the analyte expressed in the percentage. The maximum acceptable RSD % calculated based on the above eq. for an analyte concentration of 0.5 mg L^{-1} was 2.20% and for 0.05 mg L^{-1} it was 3.98%.

3. Results and Discussion

3.1. Characterization of ZnO Nano Particles

3.1.1. SEM

To study the morphological properties of the ZnO nano particles, the SEM technique was used. From the SEM image (Figure 1), it can clearly indicate that the ZnO nano particles are in homogeneous shape and size. From the SEM images observed that the ZnO nano particles were having the needles like morphology with size 50-60 nm in diameter. From the literature, it was revealed that as compared to spherical structures, needles or rod-like structures exhibit more photocatalytic activity [40,41].
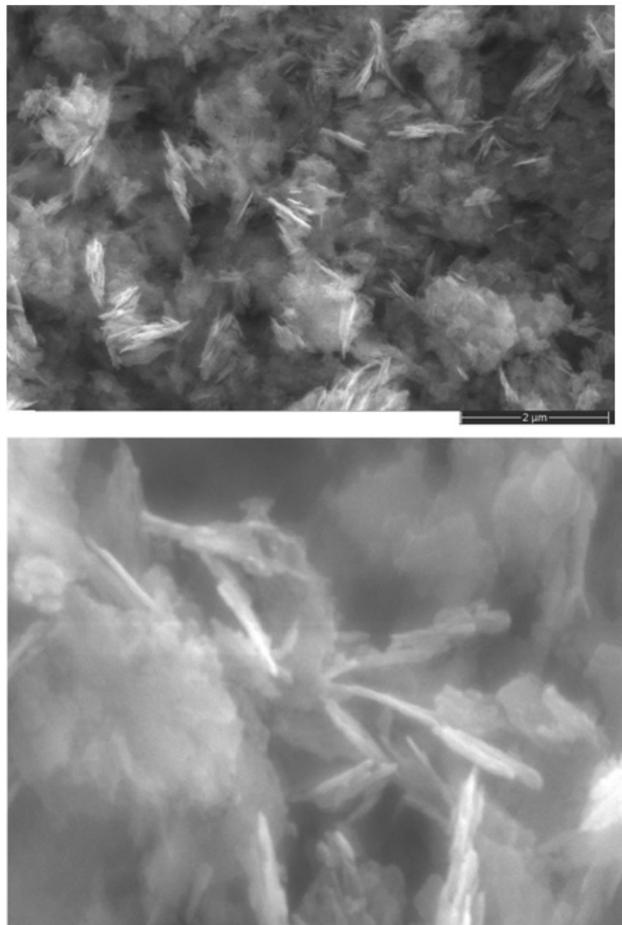

Figure 1. SEM Images of the ZnO nano particles

3.1.2. XRD

The synthesized ZnO nano particles were characterized by using X-ray diffraction technique (XRD). There are evidence and good agreement between standard diffraction peaks and the obtained peaks, which reveals that the ZnO synthesis method was successfully done. From the below figure it was revealed that diffraction peaks which are narrow and more intensive shows good crystalline nature of the ZnO, and at the bottom, the broadening peaks were indicates that the crystalline sizes are very small [42]. The graph was shown in (Figure 2).

3.1.3. FT-IR

(Figure 3) shows the FT-IR spectra of the ZnO nano particle the scanning range was 400-4000 cm^{-1}. In the spectra exhibit a strong Zn-O stretching bond was observed at 557.43 cm^{-1}, and stretching was observed at 3428 cm^{-1} corresponds to O-H Stretching bond. The above results are reliable with the literature values.
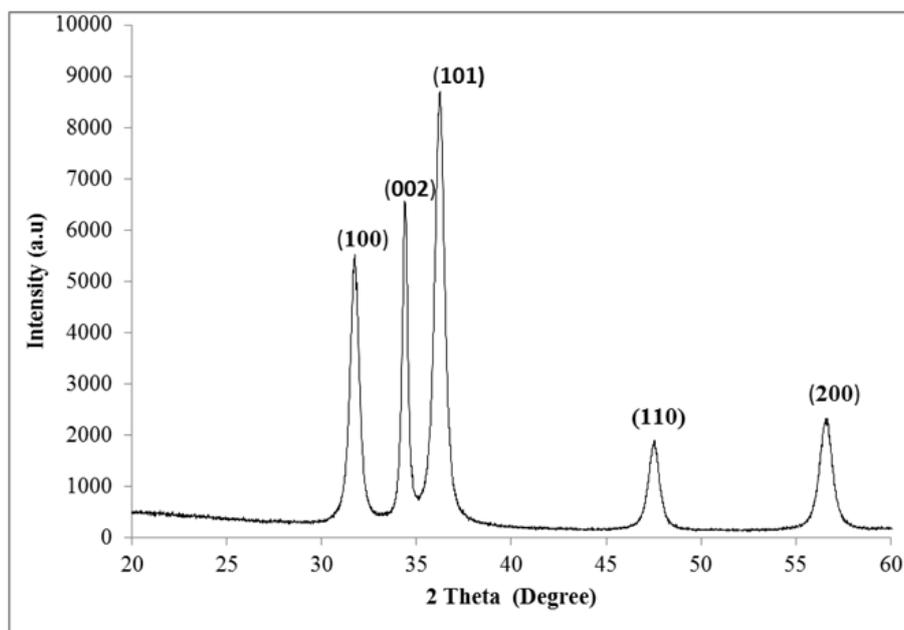
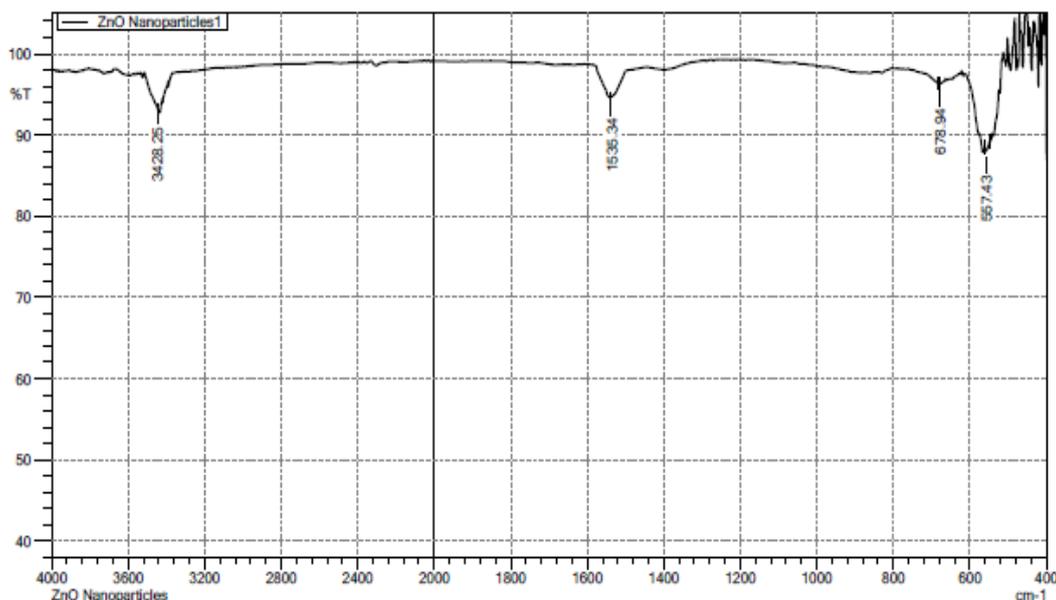**Figure 2.** XRD Image of the ZnO nano particles

Figure 3. FT-IR Image of the ZnO nano particles

3.1.4. Photo Catalysis Path Way

The ability of the semiconductor to act as a sensitizer and consequently enhances the photo degradation of the pesticides. The electronic structure is characterized by filled valence band and the empty conduction band. When ZnO is illuminated with energy higher than its band-gap energy, electron/hole pairs are produced.

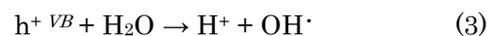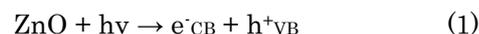$$ZnO + h\nu \rightarrow h^+ + e^-.$$

These species can either combine or react with electron donors or electron acceptors which are absorbed on the surface of the semiconductor and to produce hydroxyl radicals (OH⁺) which can promote the oxidation of the compounds.

The degradation of residues of herbicide bispyribac sodium was very slow in photolysis experiment in three different buffer solutions. In Photo catalysis, the degradation was very fast due to the photo catalyzed degradation of residues in solution was initiated by photo excitation of the metal oxide semiconductor, followed by the formation of an electron-hole pair on the surface of catalyst (Eq (1)). The high oxidative potential of the hole (h^{+VB}) in the catalyst permits the direct oxidation of residues (Herbicide) to reactive intermediates (Eq (2)). These radicals were also formed by the breakdown of water molecules (Eq. (3)) or by the reaction with OH⁻ (Eq. (4)).

The formed hydroxy radicals were very strong which leads to the complete decomposition of the organic compounds or chemicals.

$$ZnO + h\nu \rightarrow e^-_{CB} + h^+_{VB} \qquad (1)$$

$$h^{+\ VB} + compound \rightarrow compound^{\cdot} \rightarrow Oxidation \quad (2)$$

$$h^{+\ VB} + H_2O \rightarrow H^+ + OH^{\cdot} \qquad (3)$$

$$h^{+\,VB} + OH^- \rightarrow OH\cdot \qquad (4)$$

Electrons in the conduction band (e^-_{CB}) on the photo catalyst surface can reduce molecular oxygen to superoxide anion (Eq.(5)). The formed radicals in the presence of organic scavengers may form organic peroxides or hydrogen peroxides (Eq. (6)).

$$e^-_{CB} + O_2 \rightarrow O_2\cdot^- \qquad (5)$$

$$O_2\cdot^- + H_2O\cdot + H^+ \rightarrow H_2O_2 + O_2. \qquad (6)$$
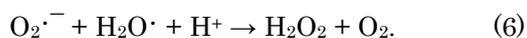
The Production of the hydroxyl radicles is due to the presence of electrons in the conduction band. The formed radicals have been indicated as the primary cause of organic matter (Eq. (7)) [43]

$$OH\cdot + compound \rightarrow degradation\ of\ the\ compound\ (7)$$

3.2. Effect of the Amount of the Catalyst

The removal efficiency increases with an increase in the amount of catalyst dosage and then stays nearly constant in a specific catalyst amount. The most effective decomposition of residues was observed at 150 mg L^{-1} of ZnO nanoparticles in photo catalysis. The reason for this observation is to be the fact that when all the herbicide molecules are adsorbed on ZnO, the addition of a higher amount of ZnO will not effect on the degradation efficiency. Due to their high surface energy to volume ratio, they tend to aggregate [44].

From (Figure 4), it can be explained that the photo degradation efficiency increases with increase in the catalyst amount up to 150 mg L^{-1} and then decreased. These observations can be explained regarding the availability of active sites on the catalyst surface and the penetration of UV light into the suspension. The total active surface area increases with increasing catalyst dosage. The optimum concentration of the nanoparticles for effective decomposition of herbicide residues was observed at 150 mg L^{-1}.
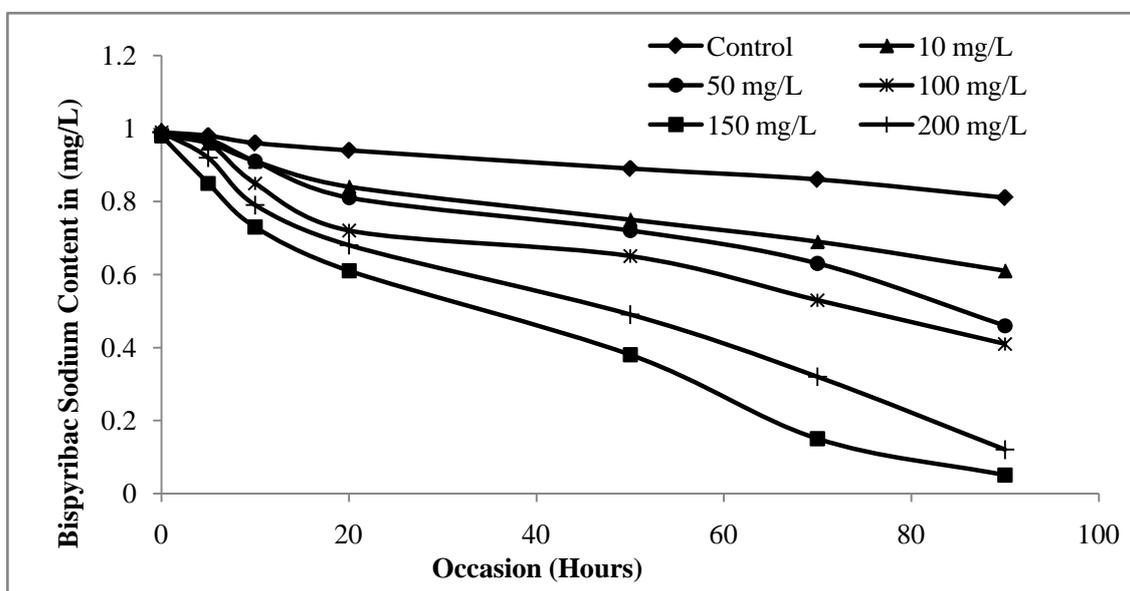

Figure 4. Effect of different amount of Catalyst used for the photo catalysis of Bispyribac Sodium
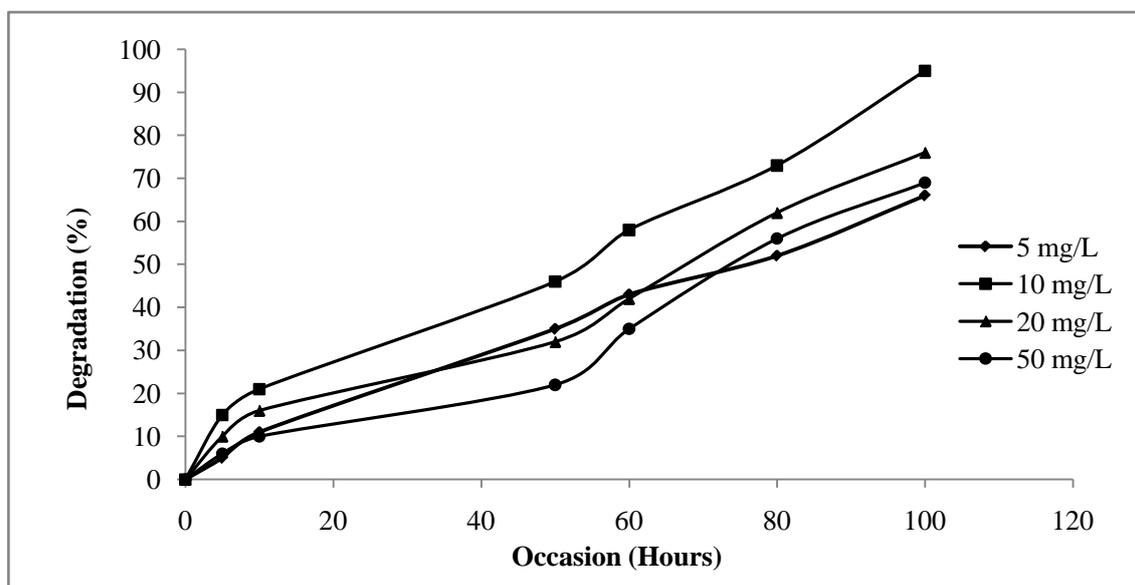

Figure 5. Effect of Initial Concentration of Bispyribac Sodium in the photo catalysis reaction. Irradiation time: 100 hours, Catalyst Concentration: 150mg L^{-1}

3.3. Effect of Initial Concentration of Compounds

The effect of initial concentration of the compounds on degradation was examined by varying the initial concentration of herbicide (5, 10, 20, and 50 mg L^{-1}) with catalyst (150 mg L^{-1}) and $Na_2S_2O_8$ (100 mg L^{-1}) under direct sunlight. The photo catalytic degradation of the bispyribac sodium was decreased 95.8% to 10.5% with increase the bispyribac sodium amount from 5 to 50 mg L^{-1} after 100 hours of continuous irradiation. The results are presented in (Figure 5). From the above results, it can be concluded that the photo degradation of the herbicide was decreased while increasing the initial concentration of the herbicide. The reason is more and more herbicide molecules were adsorbed on the surface of the catalyst ZnO and leads to the inhibition of holes or hydroxyl radicals. Similar results have been reported by the others [45].

3.4. Effect of Addition of Oxidant on Photodecomposition of Herbicide Residues

The addition of other powerful oxidizing agents, such as hydrogen peroxide and sodium persulphate to ZnO nano suspension is a very well-known and extensively studied procedure, and many cases lead to enhance the rate of the photo catalytic degradation because they trap the photogenerated electrons more efficiently than the molecular oxygen. A negative result was found [46] for the photo oxidation of the different pesticides; the addition of hydrogen peroxide does not improve the results. In fact, with an excess of peroxide, it can act as an $OH^{\bullet}$ scavenger. On the contrary, the addition of $Na_2S_2O_8$ (100 mg L^{-1}) was beneficial because (1) the oxidant strongly enhances the reaction rate and increased the number of trapped electrons (2) to generate more radicals and other oxidizing species, (3) to increase the oxidation rate of intermediate compounds. No significant differences in the reaction rates were observed when there was an increase in the concentration of the oxidant. The peroxydisulfate enhancement effect is related to both scavenging's of electrons and production of additional oxidizing species. It traps the photo generated electrons and reduces the probability of recombination with the positive holes. The addition of this inorganic oxidant produces $SO_4^{\bullet-}$ radicals which are also a strong oxidizing species (Eo= 2.7V) and more hydroxyl radicals. Due to these reasons for the reduction in treatment time, the rate of reaction increases than ZnO alone.

The degradation rate of a compound in photo catalytic oxidation of ZnO occurs by photo generated holes it is well known that oxidation rate increases when the recombination process is suppressed. Peroxydisulfate has been shown to be a more reliable and cheaper electron acceptor [47]. The results are presented in (Figure 6).
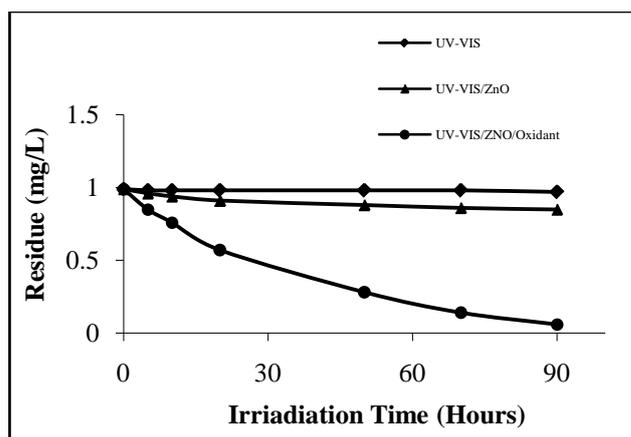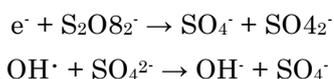
$$e^- + S_2O_8{_2}^- \rightarrow SO_4^- + SO_4{_2}^-$$

$$OH^{\cdot} + SO_4{}^{2-} \rightarrow OH^- + SO_4^-$$

Figure 6. Influence of addition of Oxidant ($Na_2S_2O_8$) to the photo catalysis reaction

3.5. Reusability of Photocatalyst

The reproducibility or reusability of a photo catalyst was studied by conducting the experiment with the same catalyst for five repeated runs. The catalyst showed excellent concordance during the experiment. The results are presented in (Figure 7).
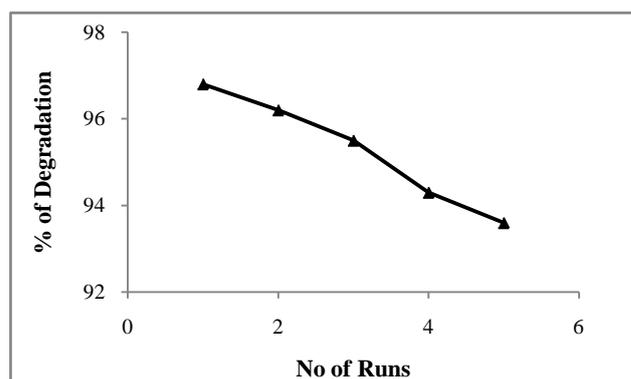

Figure 7. Reusability of the Catalyst after five successive runs

3.6. Photolysis and Photocatalysis

The photolysis of Bispyribac sodium results shows that the compound was more stable in basic water (pH 9.0) and rapidly degraded in acidic water (pH 4.0) under the influence of direct sunlight without catalyst and oxidant. The results showed that the compound was very stable in basic water and the residues were analyzed up to 375 days. In neutral water (pH 7.0), the residues went down to below detectable level in 160 days. In acidic water, the degradation was within 30 days with the half-life of around five days. In the photo catalysis experiment (With ZnO/oxidant) the residues degraded very rapidly in acidic water, i.e. DT_{50} 5.50 h and DT_{90} 18.26 h. In neutral water, the DT_{50} and DT_{90} values were 23.12 h and 76.82 h respectively. And in basic water, the DT_{50} and DT_{90} values were 63.34 h and 210.40 h respectively. The DT_{50} and DT_{90} values were calculated from the dissipation data in three different buffer solutions were presented in (Table 1 - Table 3), (Figure 8). The degradation of the residues was confirmed by LC-MS/MS, and the major transformation products identified in the water medium was presented in (Figure 9).
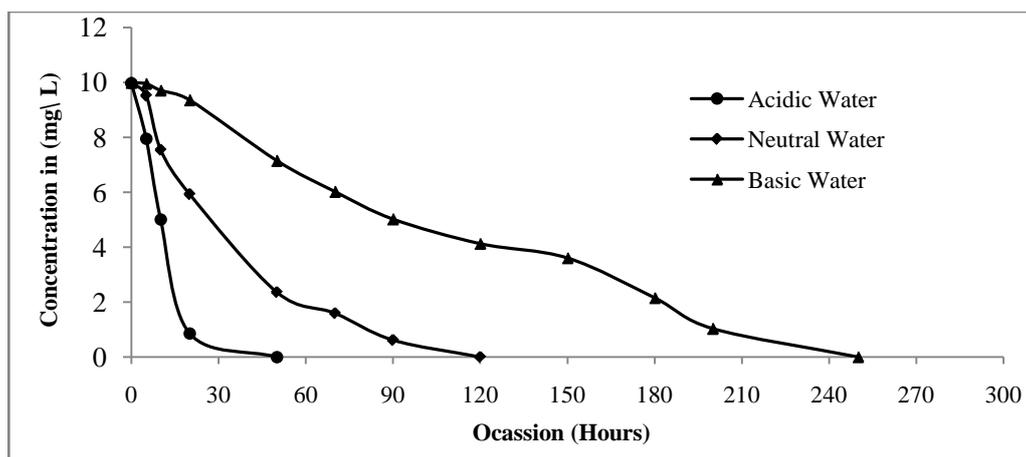
Figure 8. Dissipation of Bispyribac Sodium under sunlight with 150 mg L^{-1} catalyst and oxidant $Na_2S_2O_8$ in pH4, 7 and 9 buffers

2,6-bis(4,6-dimethoxypyrimidin-2-yloxy)benzoic acid - m/z= 430.11

sodium 2-(4,6-dimethoxypyrimidin-2-yloxy)=
-6-(4-hydroxy-6-methoxypyrimidin-2-yloxy)benzoate-
m/z= 438.08

Bispyribac Sodium - m/z = 452.09

sodium 2-(4-hydroxy-6-methoxypyrimidin-2-yloxy)-6-
hydroxybenzoate - m/z = 300.2

sodium 2-(4,6-dimethoxypyrimidin-2-yloxy)-6-
hydroxybenzoate - m/z = 314.05

2,6-dihydroxybenzoic acid
m/z = 154.03

4,6-dimethoxypyrimidin-2-ol - m/z = 156.05
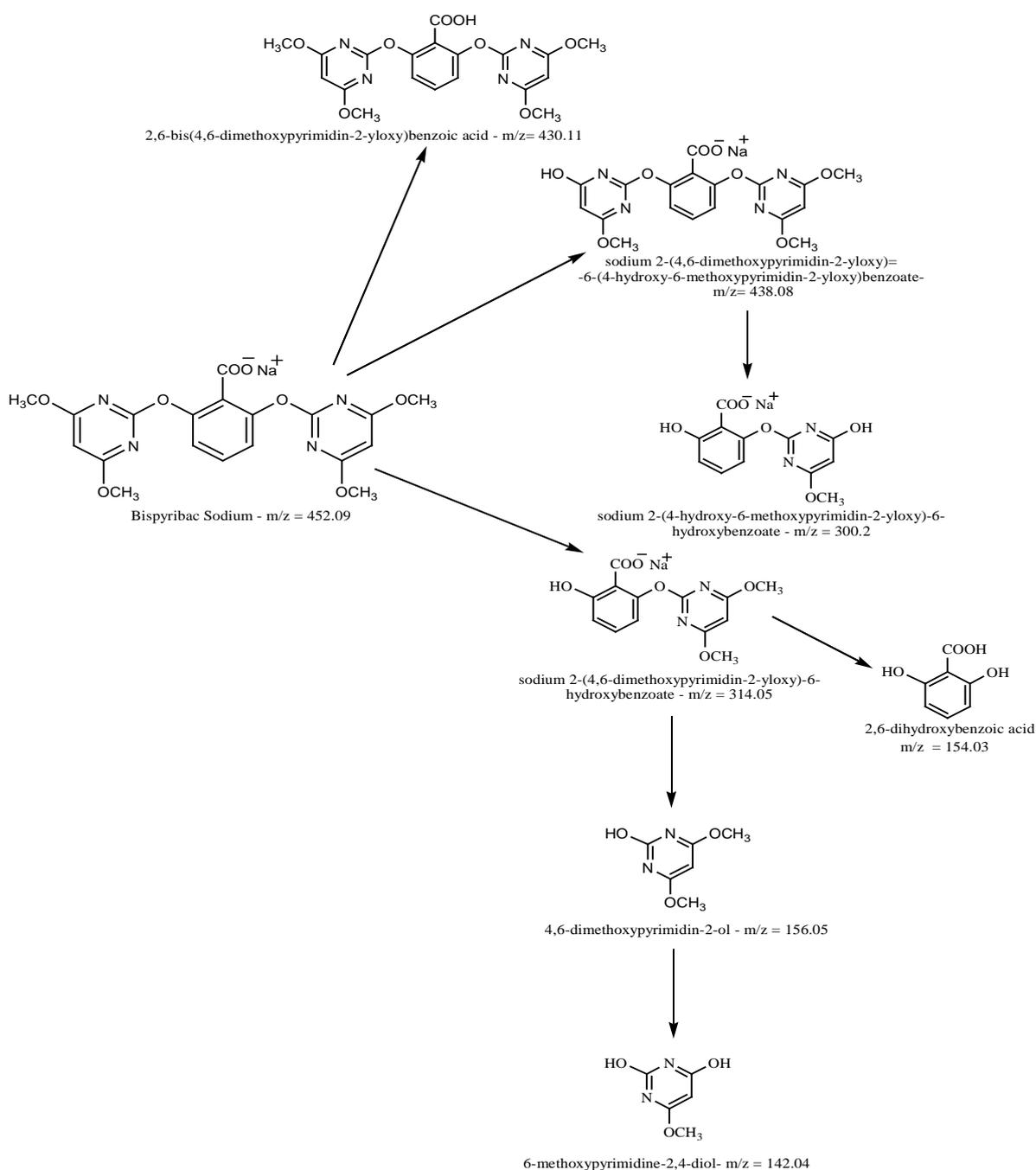
6-methoxypyrimidine-2,4-diol- m/z = 142.04

Figure 9. Major Transformation products identified in the water medium

Table 1. DT$_{50}$ values of Bispyribac Sodium in pH 4 buffer using ZnO nano Particles/Oxidant

Sampling occasion (Hours)	* Concentration (mg L^{-1})	Log of Concentration
0	9.98	0.999
5	7.96 (20.4)	0.901
10	5.01 (49.9)	0.700
20	0.86 (91.4)	-0.066
50	0.00	0.000
	Slope	-0.055
	DT$_{50}$	5.50 h
	DT$_{90}$	18.26 h

*Mean of three replicates.

Table 2. DT$_{50}$ values of Bispyribac Sodium in pH 7 buffer ZnO nano Particles/Oxidant

Sampling occasion (Hours)	* Concentration (mg L^{-1})	Log of Concentration
0	9.987	0.999
5	9.532 (4.77)	0.979
10	7.548 (24.52)	0.878
20	5.926 (40.74)	0.773
50	2.358 (76.42)	0.373
70	1.593 (84.07)	0.202
90	0.611 (93.89)	-0.214
120	0.000	0.000
	Slope	-0.013
	DT$_{50}$	23.12 h
	DT$_{90}$	76.82 h

*Mean of three replicates.

Table 3. DT$_{50}$ values of Bispyribac Sodium in pH 9 buffer using ZnO nano Particles/Oxidant

Sampling occasion (Hours)	* Concentration (mg L^{-1})	Log of Concentration
0	9.99	1.000
5	9.96 (0.4)	0.998
10	9.71 (2.9)	0.987
20	9.36 (6.4)	0.971
50	7.55 (24.5)	0.878
70	6.01 (39.9)	0.779
90	5.45 (45.5)	0.736
120	4.93 (50.7)	0.693
160	3.81(61.9)	0.581
180	1.18 (88.2)	0.072
200	0.8 (92.1)	-0.097
250	0.00	0.000
	Slope	-0.005
	DT$_{50}$	63.34 h
	DT$_{90}$	210.40 h

*Mean of three replicates.

The rate constant k [48] was calculated from the dissipation of bispyribac sodium with time using the following equation K = ln C_1/C_2/t where t is the time interval between t1 and t2 and C_1, C_2 are the concentrations of pesticides at time t_1 and t_2 respectively. The higher coefficient of correlation (R^2 = 1.000) for the least squares indicates that the degradation of bispyribac follows the first order kinetics in water. The rate constant k was calculated from the first order rate equation.

The rate constant values calculated for Bispyribac sodium under the influence of direct sun light without catalyst are; acidic Water – 0.748; Neutral water – 0.461 and in basic water - 0.585 at the tested concentration of 10 mg L^{-1} respectively. The rate constant values of photo catalytic reaction in the presence of ZnO and Oxidant are; 3.852 for acidic water, 2.530 and 2.675, in neutral and basic water respectively. This increase in the rate constant nearly five folds indicates that the zinc oxide nano particles increase the degradation rate of bispyribac sodium.

3.7. Toxicity Assessment to Green Alga (*Pseudokirchneriella subcapitata*)

In the control, the initial cell count was 1×10^4 (10000) cells/mL. The average 72 hours control cell count in the occasions 0th, 10th, 50th and 120th were 125×10^4, 127×10^4, 126×10^4 and 130×10^4 cells/mL respectively. The cells of *Pseudokirchneriella subcapitata* were increased by approximately 125, 127, 126 and 130 times in the control at 0th, 10th, 50th and 120th hours respectively(increased by more than 16 times). The percent coefficient of variation (% CV) for section by section specific growth rate in the controls (0 - 24 hours, 24 - 48 hours and 48 - 72 hours) was 15.25%, 17.60%, 18.11% and 19.26% at 0th, 10th, 50th and 120th hours respectively (less than 35% as per the OECD guideline). The percent co-efficient of variation of average specific growth rate during the whole test period (0 - 72 hours) in replicate control flasks was 1.07%, 0.98%, 1.61% and 1.10% at 0th, 10th, 50th and 120th hours respectively (less than 7 % as per the OECD guideline). These above findings validate the results of the present study.

Table 4. Percent of Inhibition of yield (%Iy) and growth rate (% Ir) at different time points

Sampling occasion (Hours)	*Percent of Inhibition	
	(%Iy)	(%Ir)
0	90.39	46.95
10	7.61	1.62
50	3.87	0.81
120	-0.13	0.0

*Mean of three replicates.

Initially (before sunlight exposure) 90.39% inhibition of yield and 46.95% of inhibition in growth rate was observed at 10.0 µg/mL concentration level. The metabolite-I [Sodium 2-(4,6-dimethoxypyrimidin-2-yloxy) -6-(4-hydroxy-6-methoxypyrimidin-2-yloxy)benzoate] was formed after 10 hours exposure of sunlight with ZnO/Na$_2$S$_2$O$_8$ nanoparticles when analyzed in HPLC and Confirmed by the LC-MS/MS analysis. The percent inhibition of yield and growth rate at 10th hour samples showed 7.61 % and 1.62 % was observed and the metabolite-II [Sodium 2-(4-hydroxy-6-methoxypyrimidin-2-yloxy)-6-hydroxybenzoate] formed after 50 hours of sunlight exposure showed the inhibition of yield was 3.87% and inhibition of growth rate was 0.81%. Compound dissipated to below detectable level at 120th hour when analyzed in HPLC and Confirmed by the LC-MS/MS analysis. Analysis of 120th hour samples showed no sign of inhibition in the yield and growth rate of green alga and the growth was on par with the control. Percentage growth inhibition and inhibition of yield were presented in (Table 4). The percentages of inhibition of the growth versus different sampling occasion were presented in (Figure 10).
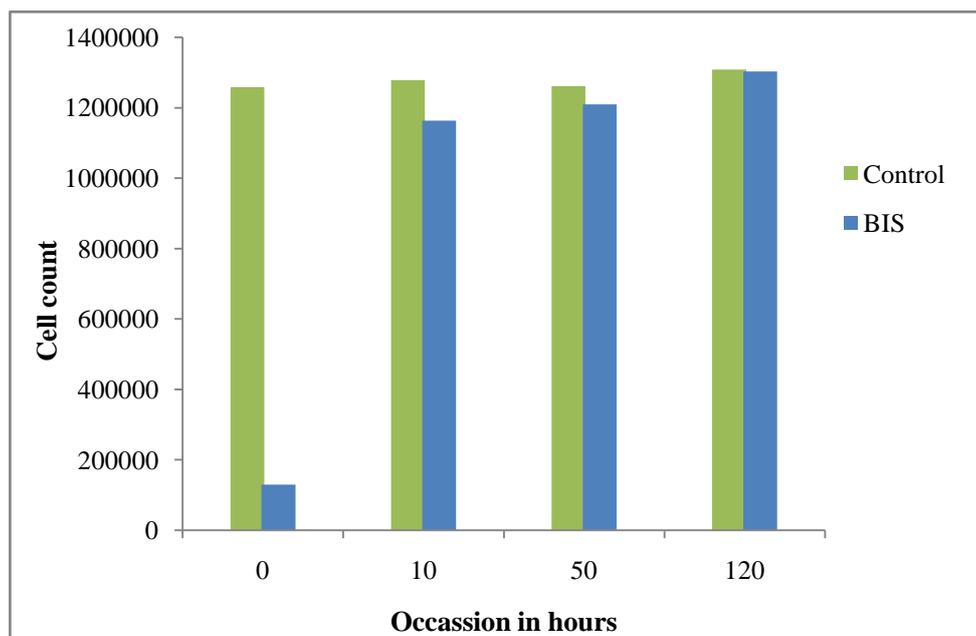
Figure 10. Percentage of Inhibition in growth of alga in control and treated samples at different Sampling occasions

From the results it was observed that during the sunlight irradiation with $ZnO/Na_2S_2O_8$ nano particles the metabolites formed in the photo catalysis showed low inhibition compared to parent bispyribac Sodium. The metabolites were not identified with equal or higher toxicity than the parent compound.

observed in (0 hours) samples. The gradual decrease in the growth inhibition was observed with increasing the irradiation time. From the above results indicate that the metabolites formed during the photo catalysis reaction were not equal or higher toxic than the parent compound to the alga.

4. Conclusions

In the present research, the herbicide bispyribac sodium was photo catalytically degraded in the presence of ZnO nano particles in three different buffer solutions of pH ranging from 4-9. The rapid degradation of the compound in photo catalysis in the presence of ZnO nano particles was obtained, the half-life ranging from 4 to 65 hours. In the photolysis process the compound was very stable; the half-life values were 5 to 107 days in different buffer solutions. The dosage of the ZnO increased, the degradation of the compound was increased up to 150 mg L^{-1}, while increasing the dose gradually decreasing the catalytic activity due to the blockage of the sunlight on the active sights of the compound. So the optimum amount of the catalyst was 150 mg L^{-1}. Based on the findings the addition of the oxidant increases the rate of the reaction. The reaction was followed by the first order kinetics. The rate of the reaction was increased up to 5 folds when compared to the photolysis reaction. From the photo catalysis, results showed that the compound was completely mineralized after 120 hours of irradiation in neutral water. The reusability of the catalyst was checked and found to be the photo catalytic activity of the catalyst up to five successive runs. The possible metabolites formed during the photo catalysis were identified by using LC-MS/MS. Five major metabolites were identified, and the toxicity of the metabolites was evaluated using the green alga as a test organism. Our experiment results confirm that the 90.39% inhibition of yield and 46.95% of inhibition in growth rate was

Acknowledgements

Conflict of Interest

No potential conflict of interest was reported by authors.

References

[1]   Abdullah, M., et al., Effects of common inorganic anions on rates of photocatalytic oxidation of organic carbon over illuminated titanium dioxide. J. Phys. Chem, 1990, 94, 6820-6825.

[2]   Conningham, J., et al., Aquatic and Surface Photochemistry. Lewis Publishers. Boca Raton. FL, 1994 Chapter 22.

[3]   Fox, M.A., Doan, K.E., Dulay, M.T. The effect of the "Inert" support on relative photocatalytic activity in the oxidative decomposition of alcohols on irradiated titanium dioxide composites. Res. Chem. Intermed, 1994, 20, 711.

[4]   Greem, K.J., Rudham, R. Photocatalytic oxidation of propan-2-ol by semiconductor–zeolite composites. J. Chem. Soc. Faraday Trans, 1993, 89, 1867.

[5]   Mattews, R.W., An adsorption water purifier with in situ photocatalytic regeneration. J. Catal, 1988, 113, 549-555.

[6]   Mattews, R.W., Response to the comment. Photocatalytic reactor design: an example of mass-transfer limitations with an immobilized. J. Phys. Chem, 1988, 92, 6853-6854.

[7]   Mattews, R.W., Purification of water with near UV illuminated suspensions of titanium dioxide. Water Research, 1990, 24, 653-600.

[8] Ollis, D.F., and Al-Ekabi, H., Photocatalytic Purification and Treatment of Water and Air (Eds.). Elsevier Sci. Publishers, Amsterdam, 1993, pp. SI 1-532.

[9] Sabate, J., et al., Comparison of TiO_2 powder suspensions and TiO_2 ceramic membranes supported on glass as photocatalytic systems in the reduction of chromium (VI). J. Mol. Catal, 1992, 71, 57-68.

[10] Sabate, J., et al., A kinetic study of the photocatalytic degradation of 3- chlorosalicylic acid over TiO_2 membranes supported on glass. J. Catal, 1991,127, 167-177.

[11] Serpone, N., and Pelizzetti, E. Photocatalysis-Fundamentals and Aplications. Interscience, 1989, New York.

[12] Xu, Y., and Chen, X, Photocatalytic reduction of dichromate over semiconductor catalysts. Chem. Ind, 1990. 15, 497-498.

[13] Ghaffarian HR, Saiedi M & Sayyadnejad M, Synthesis of ZnO nanoparticles by spray pyrolysis method, Iran. J. Chem. Chem. Eng., 2011, 30, 1-6.

[14] Sakthivel, S., et al., Solar photocatalytic degradation of azo dye: comparison of photocatalytic efficiency of ZnO and TiO_2. Solar Energy Mat. Solar Cells, 2003. 77, 65-82.

[15] Anandan, S., et al., Photocatalytic activity of La-doped ZnO for the degradation of monocrotophos in aqueous suspension. J. Mol. Catal. A Chem, 2007, 266, 149-157.

[16] Pradeep, R S., et al., Photocatalytic oxidation of phenolic compounds using zinc oxide and sulphate radicals under artificial solar light. Sep. Purific. Technol, 2010, 70, 338-344.

[17] Anđelka, T., et al., A study of the photo-catalytic degradation of methomyl by UV light. Chem. Ind. Chem. Eng. Quart, 2009, 15, 17-19.

[18] Wang, Q., Geng, B., Wang, S., ZnO/Au hybrid nanoarchitectures: wet-chemical synthesis and structurally enhanced photocatalytic performance. Environ. Sci. Technol., 2009, 43, 8968-8973.

[19] Burbano, J., et al., Evaluation of Zinc Oxide-Based Photocatalytic Degradation of a Commercial Pesticide. J. Adv. Oxid. Technol., 2008, 11, 49-55.

[20] Anandan, S., et al., Photocatalytic activity of La-doped ZnO for the degradation of monocrotophos in aqueous suspension. J. Mol. Catal. A Chem, 2007, 266, 149-157.

[21] Kamel, D., and Tahar, S., Kinetics of heterogeneous photo catalytic decomposition of 2,4-dichlorophenoxyacetic acid over titanium dioxide and zinc oxide in aqueous solution, Pest Manag. Sci, 1999, 54, 269-276.

[22] Emmanuelle, V., Corinne, E., Jean-Marc, C., Influence of pH and irradiation wavelength on the photochemical degradation of sulfonylureas. J. Photochem. Photobiol A: Chem, 2004, 163, 69-75.

[23] Emmanuelle, V., et al., Photocatalytic degradation of sulfonylurea herbicides in aqueous TiO_2. Appl. Catal. Environ, 2002, 38, 127-137.

[24] Daneshvar, N., et al., Photo-catalytic degradation of the insecticide diazinone in the presence of prepared nanocrystalline ZnO powders under irradiation of UV-C light. Sep. Purific. Technol, 2007, 58, 91-98.

[25] Umar, I.G., et al., Photocatalytic treatment of 4-chlorophenol in aqueous ZnO suspensions: Intermediates, influence of dosage and inorganic anions. J. Hazard. Mat, 2009, 168, 57-63.

[26] Young, J.J., Cynthia, S., Taein, O., Comparison of zinc oxide nanoparticles and its nano-crystalline particles on the photocatalytic degradation of methylene blue. Mat. Res. Bull, 2006, 41, 67-77.

[27] Chung-Hsin Wu, et al., Photodegradation of polychlorinated dibenzo-p-dioxins: comparison of photocatalysts. J. Hazard. Mat. 2004, 114, 191-197.

[28] Kandavelu, V., Kastien, H., Ravindranathan, T.K., Photo catalytic degradation of isothiazolin-3-ones in water and emulsion paints containing nanocrystalline TiO_2 and ZnO catalysts. Appl. Catal. B: Environ, 2004, 48, 101-111.

[29] Rabindranathan, S., Devipriya, S., Yesodharan, S., Photocatalytic degradation of phosphamidon on semiconductor oxides. J. Hazard. Mat, 2003, 29, 217-229.

[30] Daneshvar, J. N., SalariD., and Khataee,A.R., Photocatalytic degradation of azo dye acid red 14 in water on ZnO as an alternative catalyst to TiO_2. J. Photochem. Photobio. A Chem., 2004, vol. 162, 317-322.

[31] Kansal, S.K., Ali, A.H., and Kapoor,S., Photocatalytic decolorization of beibrich scarlet dye in aqueous phase using different nanophotocatalysts. Desalination, 2010, 259, 147-155.

[32] Chakrabarti, S., and Dutta, B.K., Photocatalytic degradation of model textile dyes in wastewater using ZnO as semiconductor catalyst. J. Hazard. Mater, 2004, 112, 269-278.

[33] Tan,T.K., et al., Photodegradation of Phenol Red in the Presence of ZnO Nanoparticles. World Academy of Science, Engineering and Technology, 2011, 55.

[34] Badalpoor,N., Giahi,M., and Habibi,S., Photocatalytic degradation of Lidocaine HCl using CuO/ZnO nanoparticles. Journal of Physical and Theoretical Chemistry of Islamic Azad University of Iran, 2012, 9 (1), 29-34.

[35] Pest. Management Regulatory Agency Proposed Registration Decision- PRD 2008-02, Bispyribac Sodium.

[36] Conclusion on the peer review of the pesticide risk assessment of the active substance Bispyribac, European Food Safety Authority, EFSA Journal 2010, 8(10):1692.

[37] OECD Guidelines for Testing of Chemicals (No. 301, Adopted: 17th July 1992) Ready biodegradability.

[38] M. Vafaee, M.S. Ghamsari, Preparation and Characterization of ZnO nanoparticles by a novel sol-gel route, materials Letters, 2007, 61, 3265-3268.

[39] OECD Guidelines for Testing of Chemicals (No. 201, Adopted: 7 June 1984) Alga, ''Growth Inhibition Test''.

[40] Y. Zheng, C. Chen, et al., Luminescence and Photocatalytic activity of ZnO nanocrystals: Correlation between Structure and Property. Inorg. Chem, 2007, 46, 6675- 6682.

[41] Q Wan, TH Wang, JC Zhao, Enhanced photocatalytic activity of ZnO nanotetrapods. Appl. Phys. Lett., 2005, 87: 083105-083107.

[42] EI Saeed AM, EI-Fattah MA, Azzam AM, Synthesis of ZnO nanoparticles and studying its influence on the antimicrobial, anticorrosion and mechanical behavior of polyurethane composite for surface coating. Dyes Pigment, 2015, 121: 282-9.

[43] Badalpoor N, Giahi M & Habibi S, *Journal of Physical and Theoretical Chemistry,* 9 (1) (2012), 29-34.

[44] Allen, N.S., et al., Factors affecting the interfacial adsorption of stabilizers on to titanium dioxide particles (flow microcalo-rimetry, modelling, oxidation and FT-IR studies) Nano ver-sus pigmentary grades, J. Dyes and Pigments, 2006, 70, 19/2-203.

[45] Wei, L., Shifu, Ch., Wei, Zh., Sujuan, Zh., Journal of Hazardous Materials, 2009, 164.

[46] Fenoll, S. J., Vela,N., Ruiz,E., Navarro,G, Photocatalytic degradation of eight pesticides in leaching water by use of ZnO under natural sunlight. Journal of hazardous Materials, 2009. 172, 1303-1310.

[47] Masoud Giahi, and Faegheh Ghanbari., Photocatalytic Degradation of Triton X-100 by Zinc oxide Nanoparticles. Journal of Physical and Theoretical Chemistry, 2010, 7 (3), 189-193.

[48] Ramesh A and Balasubramanian M, Kinetics and hydrolysis of fenamiphos, fipronil and triflurolin in aqueous buffer solutions, Journal of Agricultural and Food Chemistry, 1999, 47, 3367-3372.